# Part B2 - **Stability, Coupling, and Dimensions of Electromagnetic Waves**

Franc Rozman

---

## Abstract

*Part B1 introduced the electromagnetic wave as a continuous three-dimensional field structure with finite transverse organization. Part B2 develops this concept further by examining possible mechanisms for the outer boundary, radial saturation, transverse growth, interaction between neighboring structures, and experimental determination of their characteristic dimensions.*

*A possible mechanism for a sharply limited outer magnetic field is developed from Maxwell's displacement current. The model assumes a longitudinal displacement current in the inner region of the wave and an oppositely directed return contribution in an outer annular region. A smooth example is introduced in the form*

$$J_{D,z}(r,t) = J_0(1-3x^2)(1-x^2)\cos(\omega t - kz)\,, \qquad x = \frac{r}{R_{\text{out}}}$$

*which produces an azimuthal magnetic field*

$$B_\varphi(r,t) = \frac{\mu_0 J_0 R_{\text{out}}}{2} x(1-x^2)^2 \cos(\omega t - kz)$$

*The total enclosed displacement current vanishes at the outer radius, and the corresponding magnetic field decreases continuously to zero there. This provides an explicit example of how a finite transverse magnetic boundary may arise without a material wall.*

*Radial saturation is examined through the Maxwell stress tensor. For a simplified field configuration with predominantly radial electric field and azimuthal magnetic field, the radial stress component is*

$$T_{rr} = \frac{\varepsilon_0 E_r^2}{2} - \frac{B_\varphi^2}{2\mu_0}$$

*An integrated radial stress indicator is defined across the transverse section. The resulting balance condition,*

$$E_0^2 I_E = c^2 B_0^2 I_B$$

*shows that saturation depends not only on the characteristic field amplitudes but also on their radial profiles. A change in the electric-field nonlinearity can reverse the sign of the integrated radial stress indicator, providing a quantitative basis for the proposed transition from contraction through saturation to expansion.*

*The paper further considers interactions between separate saturated electromagnetic-wave structures. Ordinary overlap produces interference through linear superposition. The model proposes that sufficiently prolonged constructive overlap may generate a temporarily oversaturated common region, followed by transverse expansion and, under favorable conditions, possible structural merging. For nearly parallel structures, the overlap time increases as the convergence angle decreases, introducing a possible critical angle for reorganization.*

*For geometrically similar saturated structures, the energy-radius relation is approximated by*

$$W = C\lambda\varepsilon_0 E_0^2 R_0^2$$

*so that, at fixed wavelength and comparable saturated amplitudes,*

$$R_0 \propto \sqrt{W}$$

*Additional energy may therefore be accommodated primarily by transverse growth rather than by a permanent increase of the characteristic field amplitudes.*

*Finally, the model is connected to experiment through measurements of transverse scale, boundary thickness, convergence angle, and possible persistent restructuring after controlled two-beam overlap. Double-slit measurements are proposed as a possible method for constraining a finite transverse structural scale, while direct two-beam experiments provide a more decisive test of merging beyond conventional linear superposition.*

*The present analysis does not constitute a complete three-dimensional source-free Maxwell solution. Its purpose is to establish explicit mathematical examples, quantitative stress criteria, and experimentally testable consequences that can guide further development of the proposed electromagnetic-wave structure.*

## 1. Introduction

Part B1 introduced the electromagnetic wave as a continuous three-dimensional field structure characterized by a longitudinal wavelength and a finite transverse organization. The proposed model describes the wave through characteristic electric and magnetic field distributions, a transverse radius, and an effective radial thickness. It also introduced the possibility that electromagnetic energy may be distributed among wave structures of different transverse dimensions while maintaining approximately characteristic saturated field amplitudes.

The purpose of the present paper is to investigate the physical mechanisms that may determine the transverse boundary, stability, coupling, and measurable dimensions of such electromagnetic-wave structures.

A first question concerns the outer boundary of the wave.

If an electromagnetic wave possesses a finite transverse structure, its electric and magnetic fields must decrease sufficiently rapidly outside the region in which its energy is concentrated. The present model considers the possibility that Maxwell's displacement current

participates directly in producing such a boundary.

The displacement-current density is

$$\overrightarrow{J_D} = \varepsilon_0 \frac{\partial \vec{E}}{\partial t}.$$

Within the proposed wave structure, the dominant displacement-current contribution may be directed longitudinally through the inner part of the wave, while an outer region may contain an oppositely directed contribution. If the total enclosed displacement current approaches zero at the outer radius, the corresponding magnetic circulation may also approach zero outside the wave structure.

This provides a possible electromagnetic mechanism for a sharply bounded magnetic-field region without introducing a material boundary.

A second question concerns transverse stability.

The electric and magnetic fields need not possess identical radial profiles. In particular, the magnetic field may become strongly nonlinear near the outer boundary because it must close within the wave structure, while the electric-field profile may change as the local electromagnetic energy increases.

The model therefore investigates whether radial differences between the electric and magnetic field gradients can produce different transverse tendencies.

The electromagnetic energy densities are

$$u_E = \frac{\varepsilon_0 E^2}{2},$$

and

$$u_B = \frac{B^2}{2\mu_0}.$$

Their spatial gradients contribute to the electromagnetic stress distribution. A weak or undersaturated wave may be dominated by the nonlinear radial structure of the magnetic field, producing a tendency toward transverse contraction. At higher energy density, an increasingly nonlinear electric-field profile may oppose this tendency and eventually reverse it.

The proposed saturated state is therefore interpreted as a radial equilibrium between competing electromagnetic contributions rather than as an externally imposed field limit.

A third question concerns the interaction between separate electromagnetic-wave structures.

Because Maxwell's equations are linear in vacuum, two electromagnetic waves may pass through one another while their fields temporarily superpose. In most encounters, the overlap is expected to remain transient and the waves continue along their original propagation directions.

However, the present model examines whether sufficiently favorable encounters may produce a different outcome.

When two saturated electromagnetic-wave structures of similar wavelength, phase, polarization, and propagation direction overlap for a sufficiently long time, their combined local field may temporarily exceed the characteristic saturated state. The resulting transverse response may enlarge the common field region. If this reorganization remains small, the waves separate again. If it reaches a critical stage, the model considers the possibility that the two structures reorganize into a single broader electromagnetic-wave structure.

If the characteristic saturated field amplitudes remain approximately unchanged, conservation of energy suggests that the transverse radius of the resulting structure increases as energy is accumulated.

For geometrically similar saturated structures at a fixed wavelength, the approximate relation

$$W = C\lambda\varepsilon_0 E_0^2 R^2$$

implies

$$R \propto \sqrt{W}.$$

The merging of electromagnetic waves would therefore increase primarily the transverse dimensions of the resulting wave rather than permanently increasing its characteristic saturated field amplitudes.

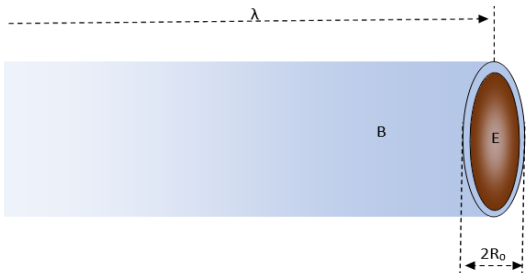


**Figure 1.** Schematic geometry of the proposed electromagnetic-wave structure. The wave propagates along the longitudinal direction with wavelength $(\lambda)$. Its transverse field distribution is assumed to have a finite characteristic diameter $(2R_0)$. The electric field $(E)$ is concentrated primarily in the inner region, while the magnetic field $(B)$ extends through the surrounding transverse region. The figure is schematic and illustrates the characteristic longitudinal and transverse dimensions of the model.

This interpretation also provides experimentally accessible questions.

The finite transverse radius of an electromagnetic wave may influence the conditions under which two separated apertures can receive coherent contributions from the same wave structure. A double-slit arrangement can therefore be used to investigate a possible upper transverse scale of the wave.

If a characteristic maximum slit separation exists beyond which the expected interference pattern disappears under otherwise unchanged conditions, the corresponding distance may provide an estimate or limit for the effective transverse radius of the electromagnetic structure.

The same arrangement may also be used to investigate the angular conditions under which separate wave structures can interact or merge.

For slit separation dd and observation distance L, a characteristic convergence angle may be approximated by

$$\theta = 2\arctan\left(\frac{d}{2L}\right).$$

For small angles,

$$\theta \approx \frac{d}{L}.$$

Measurements performed at different slit separations and observation distances may therefore provide information about both the transverse extent of the electromagnetic wave and a possible critical angular condition for prolonged coupling.

The present paper does not assume in advance that every overlap of electromagnetic waves produces permanent merging. It distinguishes ordinary transient superposition from a proposed structural reorganization that may occur only under sufficiently favorable geometric and phase conditions.

The principal objectives are therefore to examine a possible electromagnetic origin of the outer boundary, formulate a simplified mechanism of transverse saturation, investigate the conditions under which electromagnetic-wave structures may merge into wider structures, and identify experimental measurements capable of constraining their transverse radius and coupling behavior.

These questions provide a direct continuation of the conceptual framework developed in Part B1 and move the model toward experimentally testable consequences.

### 1.1. Definitions and Model Assumptions

The present paper uses a simplified structural description of an electromagnetic wave. The following definitions and assumptions are used throughout the analysis.

The electromagnetic wave is treated as a continuous three-dimensional field structure propagating predominantly along a longitudinal axis. Its longitudinal periodicity is described by the wavelength

$$\lambda$$

while its transverse organization is described by a characteristic radius.

The quantity

$$R_0$$

denotes the characteristic transverse radius of a saturated electromagnetic-wave structure. It should not be interpreted as an infinitely sharp geometrical boundary. Rather, it identifies the characteristic transverse scale of the region in which the electromagnetic field and energy are concentrated.

The quantity

$$R_{\mathrm{out}}$$

denotes the outer radius at which the field has become negligible within the proposed boundary model.

Thus, in general,

$$R_{\mathrm{out}} \geq R_0$$

The difference

$$\Delta R = R_{\mathrm{out}} - R_0$$

describes the effective thickness of the outer boundary region.

For experimental purposes, an additional radius is introduced:

$$R_{\mathrm{det}}$$

This is the radius at which the field becomes smaller than a specified experimental detection threshold. Consequently, $R_{\mathrm{det}}$ is an operational quantity and may depend on detector sensitivity.

For a sufficiently sharp boundary,

$$R_{\mathrm{det}} \approx R_0$$

may provide a useful first approximation.

The quantities

$$E_0$$

and

$$B_0$$

denote the characteristic electric- and magnetic-field amplitudes associated with the saturated state.

For propagating vacuum-field components, the approximate relation

$$E_0 \approx cB_0$$

is used.

The present paper does not require $E_0$ and $B_0$ to be universal constants for all wavelengths and all electromagnetic-wave structures. They are treated as characteristic saturated amplitudes when structures of comparable wavelength and field geometry are compared.

The quantity

W

denotes the electromagnetic energy associated with one longitudinal wave segment of length λ.

With this convention, the approximate energy relation for geometrically similar saturated structures is written as

$$W = C\lambda\varepsilon_0 E_0^2 R_0^2$$

where

C

is a dimensionless geometrical factor representing the detailed transverse

distributions of the electric and magnetic fields.

The exact value of C is not assumed in advance. It depends on the radial field profiles and can be determined only after a more complete electromagnetic field distribution is specified.

A central assumption of the model is that electromagnetic structures containing different total energies may possess similar saturated field amplitudes while differing in transverse radius. Under fixed wavelength and comparable geometry,

$$R_0 \propto \sqrt{W}$$

therefore follows from the proposed energy relation.

The model further assumes that the transverse magnetic field may be limited by a return region of displacement current near the outer boundary. In the simplified axisymmetric description, the longitudinal displacement current changes sign across the transverse section so that its integrated contribution can approach zero at the outer radius.

The electromagnetic field is assumed to propagate in source-free vacuum. No material wall or external confining structure is introduced.

The proposed saturation, finite transverse boundary, and permanent merging of electromagnetic-wave structures are model hypotheses. They are not consequences of linear Maxwell theory alone. The purpose of the following chapters is to determine whether these hypotheses can be formulated consistently and connected to experimentally measurable quantities.

Unless explicitly stated otherwise, the analytical field profiles and figures used in this paper are schematic approximations intended to describe the proposed geometry and mechanisms. They are not presented as complete three-dimensional solutions of Maxwell's equations.

# 2. Outer Boundary of the Electromagnetic Wave

Part B1 introduced the electromagnetic wave as a finite transverse field structure rather than an infinitely extended plane wave. If such a structure exists, its electric and magnetic fields must become strongly suppressed outside a characteristic transverse region.

A sharply defined outer boundary cannot be introduced as a material wall. It must arise from the electromagnetic field configuration itself.

The present model considers whether the spatial organization of Maxwell's displacement current can provide such a mechanism.

## 2.1. Displacement Current and Magnetic Circulation

In vacuum, the displacement-current density is

$$\overrightarrow{J_D} = \varepsilon_0 \frac{\partial \vec{E}}{\partial t}$$

It enters the Ampère-Maxwell equation,

$$\nabla \times \vec{B} = \mu_0 \varepsilon_0 \frac{\partial \vec{E}}{\partial t}$$

For an approximately axisymmetric electromagnetic-wave structure, let the dominant displacement-current contribution in the central region be directed along the propagation axis.

The model considers the possibility that this longitudinal displacement current does not retain the same direction throughout the complete transverse cross section. Near the outer region of the wave, the changing electric-field geometry may produce a displacement-current contribution in the opposite longitudinal direction.

The radial distribution may therefore be represented schematically as

$$J_{D,z}(r) > 0 \qquad \text{for the inner region}$$

and

$$J_{D,z}(r) < 0 \qquad \text{for an outer annular region}$$

The signs reverse periodically with the electromagnetic oscillation, but the inner and outer contributions remain oppositely directed at a given phase.

This counter-directed outer contribution is important because the magnetic field produced by the displacement current depends on the total current enclosed within a given radius.

For an approximately axisymmetric configuration,

$$2\pi r B_{\varphi}(r,t) = \mu_0 I_D(r,t)$$

where

$$I_D(r,t) = 2\pi \int_0^r J_{D,z}(r',t)\; r'\, dr'$$

Consequently,

$$B_{\varphi}(r,t) = \frac{\mu_0}{r} \int_0^r J_{D,z}(r',t)\; r'\, dr'$$

The magnetic field at a given radius is therefore determined by the accumulated displacement-current contribution inside that radius.

### 2.2. Physical Status of the Displacement-Current Field

The proposed electromagnetic-wave model assigns a fundamental physical role to three interacting electromagnetic contributions: the electric field E, the magnetic field B, and the displacement-current field J.

In conventional Maxwell electrodynamics, the displacement-current density is defined by

$$J_p = \varepsilon_0 \frac{\partial E}{\partial t}.$$

The present model retains this relation but explores the additional hypothesis that the displacement-current structure possesses its own identifiable energy, momentum, and dynamical motion within the electromagnetic wave.

The total energy of a finite electromagnetic-wave structure is represented provisionally as

$$W = W_E + W_B + W_J.$$

Here, $W_J$ denotes the proposed energy associated with the displacement-current structure. It is not identified with an additional conventional Maxwell energy term; its independent definition and consistency with energy conservation remain to be established.

During propagation, the three contributions may exchange energy while the total energy of an isolated wave structure remains conserved:

$$dW_E + dW_B + dW_J = 0.$$

The model therefore distinguishes conservation of total electromagnetic energy from the instantaneous distribution of energy among its internal components.

The displacement-current structure is also assigned a possible momentum contribution and a characteristic velocity. These quantities require their own dynamical description and cannot be inferred from the sign of the displacement-current density alone.

In particular, a negative displacement-current density does not necessarily indicate material motion opposite to the direction of wave propagation. The direction of the current, the velocity of its spatial pattern, and the velocity of any proposed physical carrier must be distinguished.

This distinction becomes essential when an electromagnetic wave propagates through an external magnetic field. If the proposed displacement-current structure possesses an independent magnetic response, that response must be formulated through an explicit interaction law consistent with conservation of energy and momentum.

The physical interpretation advanced here is therefore a foundational hypothesis of the proposed wave model. Its validation requires a self-consistent three-dimensional field solution, an explicit displacement-current

energy density, and a corresponding dynamical equation.

### 2.3. Cancellation of the External Magnetic Field

Suppose the positive displacement-current contribution in the inner region is balanced by the oppositely directed contribution in the outer region.

At the outer radius $R_{\text{out}}$, the condition is

$$\int_0^{R_{\text{out}}} J_{D,z}(r,t)\; r\, dr = 0$$

Under the assumed axisymmetric geometry, this gives

$$B_\varphi(R_{\text{out}}, t) = 0$$

If no further displacement-current contribution exists outside this radius, the enclosed total remains zero and the corresponding azimuthal magnetic field also vanishes:

$$B_\varphi(r,t) = 0, \qquad r > R_{\text{out}}$$

This provides a possible electromagnetic mechanism for producing a strongly limited outer magnetic field without introducing a physical boundary.

The external field does not disappear because it has been absorbed. Instead, the magnetic circulation produced by the central displacement current is progressively cancelled by the oppositely directed displacement current in the outer annular region.

### 2.4. Simple Two-Region Model

The principle can be illustrated by the simplest radial model.

Let the central displacement-current density be approximately constant,

$$J_{D,z} = J_0, \qquad 0 \le r < R$$

and let an oppositely directed displacement current occupy the outer annulus,

$$J_{D,z} = -\beta J_0, \qquad R \le r < R_{\text{out}}$$

The total current through the central region is

$$I_{\text{inner}} = \pi R^2 J_0$$

The contribution of the outer annulus is

$$I_{\text{outer}} = -\pi(R_{\text{out}}^2 - R^2)\beta J_0$$

Cancellation at the outer boundary requires

$$I_{\text{inner}} + I_{\text{outer}} = 0$$

This gives

$$\beta = \frac{R^2}{R_{\text{out}}^2 - R^2}$$

The result shows that a thinner outer return region requires a larger oppositely directed displacement-current density.

The corresponding magnetic field in the central region increases approximately linearly with radius,

$$B_\varphi(r) = \frac{\mu_0 J_0 r}{2}, \qquad r < R$$

Within the outer annulus, the accumulated return current progressively reduces the magnetic field.

For

$$R \le r < R_{\text{out}}$$

the field becomes

$$B_\varphi(r) = \frac{\mu_0 J_0}{2r}[R^2 - \beta(r^2 - R^2)]$$

At the outer boundary, substitution of the cancellation condition gives

$$B_\varphi(R_{\text{out}}) = 0$$

Thus, even this simple model produces a magnetic field that reaches a maximum near the characteristic radius and then falls rapidly to zero within the outer return region.

### 2.5. Sharpness of the Boundary

The outer boundary can become increasingly sharp if the oppositely directed displacement current is concentrated into a narrow annular region.

Let

$$R_{\text{out}} = R + \Delta R$$

The relative return-current density is then

$$\beta = \frac{R^2}{(R+\Delta R)^2 - R^2}$$

For

$$\Delta R \ll R$$

this becomes approximately

$$\beta \approx \frac{R}{2\Delta R}$$

Thus, reducing the width of the return region requires a corresponding increase in the local displacement-current density.

The model therefore does not imply that the outer boundary can become arbitrarily thin without consequence. A sharper boundary requires a more strongly concentrated temporal variation of the electric field.

Nevertheless, the mechanism permits the magnetic field to become strongly suppressed over a relatively narrow transverse region.

This provides a possible explanation for how an electromagnetic wave may maintain a well-defined transverse extent during long-distance propagation without continuously dispersing its energy into the surrounding space.

**2.6. A Smooth Return-Current Profile**

The piecewise-constant model introduced in Section 2.3 demonstrates the cancellation principle, but a physical electromagnetic field should vary smoothly across the transverse section.

A simple smooth example can be constructed by introducing the dimensionless radius

$$x = \frac{r}{R_{\text{out}}}, \qquad 0 \le x \le 1$$

and choosing the longitudinal displacement-current density in the form

$$J_{D,z}(r,t) = J_0(1-3x^2)(1-x^2)\cos(\omega t - kz)$$

This profile is positive in the inner region, changes sign at an intermediate radius, becomes negative in the outer annular region, and finally approaches zero smoothly at the outer boundary.

At the axis,

$$J_{D,z}(0,t) = J_0\cos(\omega t - kz)$$

The sign reversal occurs when

$$1 - 3x^2 = 0$$

which gives

$$x = \frac{1}{\sqrt{3}} \approx 0.577$$

Thus,

$$J_{D,z} > 0 \qquad 0 < x < \frac{1}{\sqrt{3}}$$

while

$$J_{D,z} < 0 \qquad \frac{1}{\sqrt{3}} < x < 1$$

At the outer boundary,

$$J_{D,z}(R_{\text{out}}, t) = 0$$

because of the factor $(1-x^2)$.

The corresponding azimuthal magnetic field follows from the Ampère-Maxwell relation,

$$B_\varphi(r,t) = \frac{\mu_0}{r}\int_0^r J_{D,z}(r',t)\; r'\, dr'$$

Since

$$(1-3x^2)(1-x^2) = 1 - 4x^2 + 3x^4$$

the radial integral becomes

$$\int_0^x x'(1 - 4x'^2 + 3x'^4)\; dx' = \frac{x^2}{2}(1-x^2)^2$$

and therefore

$$B_\varphi(r,t) = \frac{\mu_0 J_0 R_{\text{out}}}{2} x(1-x^2)^2\cos(\omega t - kz)$$

This field is zero on the axis,

$$B_\varphi(0,t) = 0$$

rises to a maximum inside the structure, and decreases continuously toward the outer boundary.

The maximum occurs when

$$\frac{d}{dx}[x(1-x^2)^2] = 0$$

which gives the internal maximum at

$$x = \frac{1}{\sqrt{5}} \approx 0.447$$

At the outer radius,

$$B_\varphi(R_{\text{out}}, t) = 0$$

The total enclosed displacement current also vanishes:

$$\int_0^{R_{\text{out}}} J_{D,z}(r,t)\; r\, dr = 0$$

Consequently, if no additional displacement current exists outside the structure, the same axisymmetric relation gives

$$B_\varphi(r,t) = 0, \qquad r > R_{\text{out}}$$

The radial sequence produced by this example is therefore

$$r = 0: \quad B_\varphi = 0$$

$$r \approx 0.447 R_{\text{out}}: \quad B_\varphi = B_{max}$$

$$r \approx 0.577 R_{\text{out}}: \quad J_{D,z} \text{ changes sign}$$

and

$$r = R_{\text{out}}: \quad J_{D,z} = 0, \quad B_\varphi = 0$$

This smooth example therefore reproduces the essential boundary mechanism proposed by the model: an inner longitudinal displacement current is balanced by an oppositely directed outer return region, causing the magnetic field to fall continuously to zero at the outer radius.

Because

$$J_{D,z} = \varepsilon_0 \frac{\partial E_z}{\partial t}$$

one compatible longitudinal electric-field profile is

$$E_z(r,t) = \frac{J_0}{\varepsilon_0 \omega}(1-3x^2)(1-x^2)\sin(\omega t - kz)$$

Thus, the same smooth radial structure that produces the return displacement current can be generated by a corresponding spatial dependence of the longitudinal electric field.

This example is not presented as a complete three-dimensional propagating Maxwell solution. Its purpose is narrower: to show explicitly that a smooth radial displacement-current distribution can contain an inner current, an outer return region, zero total enclosed displacement current, and a magnetic field that continuously approaches zero at the outer boundary.

The proposed return-current profile provides a mathematically consistent cancellation of the enclosed longitudinal displacement current and the corresponding azimuthal magnetic field at the outer radius.

This result establishes a possible geometrical mechanism for suppressing the external magnetic field without introducing a material boundary. However, the complete propagating electromagnetic structure must also satisfy Faraday's law, the electric and magnetic divergence conditions, and electromagnetic momentum conservation.

The present calculation therefore establishes the cancellation mechanism within the simplified axisymmetric model.

**2.7. Relation to the Electric Field**

The displacement current is generated by the temporal variation of the electric field.

Therefore, an oppositely directed outer displacement current requires a corresponding change in the temporal behavior of the electric-field components.

The outer magnetic boundary cannot be considered independently of the electric-field geometry.

In an axisymmetric description without free charge, the electric field must satisfy

$$\nabla \cdot \vec{E} = 0$$

For radial and longitudinal components,

$$\frac{1}{r}\frac{\partial(rE_r)}{\partial r} + \frac{\partial E_z}{\partial z} = 0$$

This relation connects the radial electric field directly to the longitudinal variation of the field associated with the displacement current.

If the integrated longitudinal contribution vanishes at the outer boundary, the radial electric field may also approach zero there under suitable field geometry.

The same structural condition can therefore contribute to the suppression of both the external magnetic field and the external radial electric field.

A complete demonstration requires a self-consistent solution of all Maxwell equations, but the integral cancellation mechanism already provides a physically motivated route toward a sharply limited electromagnetic-wave boundary.

**2.8. Effective Outer Radius**

The characteristic radius R and the outer radius $R_{\mathrm{out}}$ should be distinguished.

The radius R describes the region in which the magnetic field reaches its characteristic maximum or where electromagnetic energy is strongly concentrated.

The outer radius $R_{\mathrm{out}}$ describes the distance at which the field has become negligible.

For experimental purposes, it may be useful to define an operational radius $R_{\mathrm{det}}$ at which the field amplitude falls below the sensitivity of a particular measurement.

For example,

$$B\left(R_{1\backslash\%}\right) = 0.01B_0$$

The corresponding radius $R_{1\backslash\%}$ defines a practical one-percent boundary.

If the return-current region is sufficiently narrow, $R_{1\backslash\%}$ may lie very close to $R_{\mathrm{out}}$.

This distinction will become important when the transverse dimensions of electromagnetic waves are investigated experimentally using interference and double-slit arrangements.

**2.9. Physical Significance of a Limited Outer Field**

A strongly limited transverse field has several consequences for the proposed electromagnetic-wave model.

First, it allows the wave to retain a finite transverse concentration of energy during propagation.

Second, it provides a geometrical meaning to the characteristic radius R and to an experimentally defined outer radius.

Third, it allows separate electromagnetic-wave structures to pass through regions of space without necessarily interacting strongly unless their transverse field regions overlap.

Finally, the existence of a well-defined outer boundary makes it possible to investigate the transverse dimensions of electromagnetic waves experimentally.

The next chapter examines a related question: how differences between the radial nonlinearities of the electric and magnetic fields may produce inward or outward electromagnetic tendencies and thereby establish a dynamically saturated transverse structure. [1] [2]

## 3. Saturation and Radial Stability

Part B1 introduced the possibility that an electromagnetic-wave structure may possess a characteristic saturated state in which its transverse dimensions remain approximately stable during propagation.

The present chapter develops a simplified mechanism for such radial stability.

The central idea is that the electric and magnetic fields need not possess identical radial profiles. Near the outer boundary, the magnetic field becomes strongly nonlinear because it is forced toward zero by the return displacement-current structure described in Section 2. The electric-field profile may also become increasingly nonlinear as the local electromagnetic energy density rises.

The relative radial nonlinearities of the two fields can therefore change the direction of the electromagnetic radial tendency.

### 3.1. Radial Energy Densities

The electric and magnetic energy densities in vacuum are

$$u_E = \frac{\varepsilon_0 E^2}{2}$$

and

$$u_B = \frac{B^2}{2\mu_0}$$

Their radial derivatives are

$$\frac{du_E}{dr} = \varepsilon_0 E \frac{dE}{dr}$$

and

$$\frac{du_B}{dr} = \frac{B}{\mu_0}\frac{dB}{dr}$$

These gradients describe how rapidly the electromagnetic energy distribution changes across the transverse section of the wave.

The model does not assume that the electric and magnetic gradients are identical. Their difference becomes especially important near the outer part of the wave structure.

### 3.2. Electromagnetic Stress and Radial Tendency

For a configuration in which the electric field is predominantly radial and the magnetic field predominantly transverse or azimuthal, the radial component of the Maxwell stress tensor contains contributions of opposite character from the electric and magnetic fields.

A simplified radial stress expression may be written as

$$T_{rr} \approx \frac{\varepsilon_0 E^2}{2} - \frac{B^2}{2\mu_0}$$

Its radial variation is then approximately

$$\frac{dT_{rr}}{dr} \approx \varepsilon_0 E \frac{dE}{dr} - \frac{B}{\mu_0}\frac{dB}{dr}$$

This relation provides a simple way of comparing the influence of the two field profiles.

The present model interprets the relative magnitudes of these terms as an indicator of the radial electromagnetic tendency.

When the magnetic contribution dominates, the transverse structure tends to contract.

When the electric contribution dominates, the transverse structure tends to expand.

The saturated state corresponds to an approximate balance between the two.

### 3.3. Undersaturated Electromagnetic Wave

Consider first an electromagnetic wave whose electric-field distribution remains relatively smooth across most of the transverse section.

The electric field may be represented schematically by a nearly linear profile, while the magnetic field becomes increasingly nonlinear near the outer boundary because it must fall toward zero outside the wave structure.

Thus,

$$\left|\frac{dB}{dr}\right|$$

may become large in the boundary region even when

$$\left|\frac{dE}{dr}\right|$$

remains comparatively small.

The magnetic contribution to the radial stress gradient may then dominate:

$$\frac{B}{\mu_0}\left|\frac{dB}{dr}\right| > \varepsilon_0 E\left|\frac{dE}{dr}\right|$$

The model associates this condition with an inward radial tendency.

The electromagnetic-wave structure therefore tends to contract.

As the transverse radius decreases, the same electromagnetic energy becomes distributed over a smaller effective cross section. The characteristic field amplitudes consequently increase.

The contraction can therefore move an initially weak or undersaturated wave toward a more strongly concentrated state.

### 3.4. Increasing Nonlinearity of the Electric Field

As the electromagnetic energy density increases, the electric-field profile need not preserve its original approximately linear form.

The model proposes that the electric field becomes increasingly nonlinear, particularly in the outer part of the transverse structure.

This change increases the magnitude of

$$\varepsilon_0 E\left|\frac{dE}{dr}\right|$$

relative to the magnetic contribution.

At sufficiently high energy density, the electric term can become comparable to the magnetic term.

The transverse contraction then weakens.

A further increase in the nonlinear electric-field contribution may reverse the radial tendency completely.

### 3.5. Saturated State

The saturated state is defined as the condition at which the competing radial contributions approximately balance.

The local equilibrium condition may be written as

$$\varepsilon_0 E\left|\frac{dE}{dr}\right| \approx \frac{B}{\mu_0}\left|\frac{dB}{dr}\right|$$

At this condition, the electromagnetic-wave structure has no dominant tendency toward either contraction or expansion.

Its characteristic transverse radius is denoted by

$$R = R_0$$

The corresponding characteristic field amplitudes are denoted by

$$E = E_0$$

and

$$B = B_0$$

For the propagating components, the approximate vacuum relation remains

$$E_0 \approx cB_0$$

The saturated state should therefore be interpreted as a geometrical and dynamical equilibrium of the transverse field distributions rather than as a fundamental upper limit on electromagnetic amplitude imposed by Maxwell's equations.

### 3.6. Oversaturated Electromagnetic Wave

Suppose additional energy is transferred into an already saturated electromagnetic-wave structure while its transverse dimensions cannot adjust instantaneously.

The local electric-field profile may become more strongly nonlinear.

The electric contribution to the radial stress gradient can then exceed the magnetic contribution:

$$\varepsilon_0 E\left|\frac{dE}{dr}\right| > \frac{B}{\mu_0}\left|\frac{dB}{dr}\right|$$

The model associates this condition with an outward radial tendency.

The transverse structure therefore begins to expand.

As the radius increases, the electromagnetic energy becomes distributed over a larger cross-sectional region. The characteristic field amplitudes decrease toward their saturated values.

The proposed mechanism therefore produces a restoring response around the saturated state.

The longitudinal component $E_z$ introduced in Section 2.5 generates the longitudinal displacement current responsible for the magnetic boundary. A complete divergence-free three-dimensional field also requires transverse electric-field components. In the present radial-stability analysis, $E_r$ represents the dominant transverse electric component relevant to radial Maxwell stress. The simplified $E_z$ and $E_r$ profiles are not yet combined into a complete Maxwell solution.

**3.7. Integrated Radial Maxwell Stress**

A more quantitative estimate of radial stability can be obtained from the Maxwell stress tensor.

For a simplified configuration in which the electric field is predominantly radial and the magnetic field predominantly azimuthal, the radial stress component may be written as

$$T_{rr} = \frac{\varepsilon_0 E_r^2}{2} - \frac{B_\varphi^2}{2\mu_0}$$

The electric and magnetic contributions therefore enter the radial stress with opposite signs.

To characterize the complete transverse cross section, define the integrated radial stress indicator

$$\Sigma_r = 2\pi \int_0^{R_{\text{out}}} T_{rr}(r)\ r\ dr$$

Introducing the dimensionless radius

$$x = \frac{r}{R_{\text{out}}}$$

the electric and magnetic fields can be written as

$$E_r(x) = E_0 e(x)$$

and

$$B_\varphi(x) = B_0 b(x)$$

where $e(x)$ and $b(x)$ describe the normalized radial profiles.

The integrated radial stress then becomes

$$\Sigma_r = \pi R_{\text{out}}^2 \varepsilon_0 [E_0^2 I_E - c^2 B_0^2 I_B]$$

where

$$I_E = \int_0^1 e^2(x) x\ dx$$

and

$$I_B = \int_0^1 b^2(x) x\ dx$$

The quantities $I_E$ and $I_B$ therefore measure the effective radial contributions of the electric and magnetic field distributions.

The integrated radial stress indicator provides a measure of the relative electric and magnetic contributions across the transverse field structure. However, it should be distinguished from the complete radial electromagnetic force balance.

In cylindrical coordinates, the radial divergence of the Maxwell stress tensor also contains contributions from the azimuthal stress and possible longitudinal variations:

$$(\nabla \cdot T)r = \frac{\partial Trr}{\partial r} + \frac{T_{rr} - T_{\varphi\varphi}}{r} + \frac{\partial T_{rz}}{\partial z}$$

For the simplified field configuration considered here, with only radial electric and azimuthal magnetic components, $T_{\varphi\varphi} = -T_{rr}$ and $T_{rz} = 0$. The corresponding radial stress divergence therefore becomes

$$(\nabla \cdot T)r = \frac{\partial Trr}{\partial r} + \frac{2T_{rr}}{r}$$

Consequently, the integrated balance condition introduced below is interpreted as a geometrical stress indicator rather than a complete proof of dynamical equilibrium. The existence of a stable saturated radius additionally requires a restoring response consistent with the full electromagnetic momentum balance.

A possible saturated radial state is obtained when the integrated contributions balance:

$$\Sigma_r = 0$$

which gives

$$E_0^2 I_E = c^2 B_0^2 I_B$$

or equivalently

$$\frac{E_0}{cB_0} = \sqrt{\frac{I_B}{I_E}}$$

This relation provides a quantitative form of the saturation condition.

The saturated state is therefore determined not only by the characteristic amplitudes $E_0$ and $B_0$, but also by the radial shapes of the electric and magnetic fields.

If

$$E_0^2 I_E < c^2 B_0^2 I_B$$

the magnetic contribution dominates the integrated radial stress.

If

$$E_0^2 I_E > c^2 B_0^2 I_B$$

the electric contribution dominates.

Within the present model, these two regimes are interpreted as indicators of an inward or outward radial tendency.

The balance between them defines the proposed saturated configuration.

**3.8. Example of Stress Reversal**

The magnetic profile obtained from the smooth return-displacement-current model of Section 2.5 provides a convenient example.

Its normalized form may be written as

$$b(x) = \frac{25\sqrt{5}}{16} x(1 - x^2)^2$$

The normalization is chosen so that

$$b_{max} = 1$$

The magnetic field reaches its maximum at

$$x = \frac{1}{\sqrt{5}}$$

and approaches zero smoothly at the outer boundary.

For this profile,

$$I_B = \int_0^1 b^2(x) x \, dx = \frac{625}{3072}$$

or numerically,

$$I_B \approx 0.203$$

To examine the influence of electric-field nonlinearity, consider the family

$$e_n(x) = \frac{x(1 - x^n)}{M_n}$$

where $M_n$ normalizes the maximum electric-field amplitude to unity.

The maximum occurs at

$$x_m = \left(\frac{1}{n+1}\right)^{1/n}$$

and therefore

$$M_n = \frac{n}{n+1}\left(\frac{1}{n+1}\right)^{1/n}$$

The corresponding electric contribution is

$$I_E(n) = \int_0^1 e_n^2(x) x \, dx$$

which gives

$$I_E(n) = \frac{1}{M_n^2}\left[\frac{1}{4} - \frac{2}{n+4} + \frac{1}{2n+4}\right]$$

For several representative values,

$$I_E(1) \approx 0.267$$

$$I_E(2) \approx 0.281$$

and

$$I_E(4) \approx 0.291$$

Thus, increasing the radial nonlinearity of the electric field increases its integrated radial stress contribution.

The saturation criterion becomes

$$E_0^2 I_E(n) = c^2 B_0^2 I_B$$

This demonstrates that a change in the electric-field profile can alter the sign of the integrated radial stress even when the magnetic boundary profile remains unchanged.

For example, if

$$\frac{cB_0}{E_0} = 1.18$$

the effective magnetic contribution is approximately

$$\left(\frac{cB_0}{E_0}\right)^2 I_B \approx 0.283$$

For n=1,

$$I_E(1) \approx 0.267 < 0.283$$

and the magnetic contribution dominates.

For n=4,

$$I_E(4) \approx 0.291 > 0.283$$

and the electric contribution dominates.

The example therefore shows explicitly that a sufficiently strong change in the radial electric-field distribution can reverse the sign of the integrated radial stress.

Within the proposed model, this provides a quantitative mechanism for the transition

$$\text{contraction} \rightarrow \text{saturation} \rightarrow \text{expansion}$$

as the electromagnetic energy density and field geometry change.

The calculation does not constitute a complete dynamical solution of radial stability. A full treatment must include all components of the Maxwell stress tensor together with electromagnetic momentum conservation and the time dependence of the complete three-dimensional field.

Nevertheless, the result demonstrates that the proposed saturation mechanism can be expressed as a definite quantitative balance between electric and magnetic radial stress contributions.

### 3.9. Restoring Stability Around the Saturated Radius

The proposed saturation mechanism is based on a restoring radial response to small deviations from the equilibrium radius $R_0$.

Consider a saturated electromagnetic-wave structure with approximately constant total energy.

If its transverse radius increases slightly above $R_0$, the electromagnetic energy becomes distributed over a larger transverse region. The characteristic field amplitudes decrease, and the electric-field profile is assumed to become less nonlinear.

Under these conditions, the magnetic contribution to the radial stress balance becomes relatively more significant. The model consequently predicts an inward radial response that tends to reduce the radius toward its equilibrium value.

Conversely, if the transverse radius decreases below $R_0$, the electromagnetic energy density increases. The electric-field profile is assumed to become more strongly nonlinear, increasing its contribution to the radial stress balance.

The resulting outward radial response tends to restore the original transverse dimension.

The proposed restoring behavior can be summarized by

$$R > R_0 \quad \Rightarrow \quad F_r < 0$$

$$R < R_0 \quad \Rightarrow \quad F_r > 0$$

where $F_r$ denotes the effective radial response derived from the complete electromagnetic momentum balance, with the outward direction taken as positive.

A stable equilibrium requires

$$F_r(R_0) = 0$$

and, for small radial perturbations,

$$\left.\frac{dF_r}{dR}\right|_{R_0} < 0$$

The integrated stress analysis of Sections 3.7 and 3.8 demonstrates that changes in the relative electric and magnetic field profiles can reverse the sign of a radial stress indicator. The present model proposes that these changes occur in response to variations in electromagnetic energy density and transverse radius.

The resulting restoring mechanism is therefore a working hypothesis for transverse stability. Its quantitative confirmation requires a complete electromagnetic momentum balance and a self-consistent description of how the field profiles evolve during radial perturbations.

**3.10. Saturation and Wave Energy**

The saturated state does not require all electromagnetic waves to contain the same energy.

If the characteristic saturated amplitudes remain approximately equal, different energies may be accommodated through different transverse dimensions.

For geometrically similar saturated structures,

$$W = C\lambda\varepsilon_0 E_0^2 R_0^2$$

and therefore

$$R_0 \propto \sqrt{W}$$

at fixed wavelength and comparable field geometry.

A wave containing more energy can consequently possess a larger saturated transverse radius while maintaining approximately the same characteristic amplitudes.

This relation becomes important when separate electromagnetic-wave structures overlap and possibly combine.

**3.11. Scope of the Saturation Mechanism**

The present treatment does not constitute a complete three-dimensional Maxwell solution of a self-confined electromagnetic wave.

Instead, it identifies a simpler physical mechanism that can be tested and developed further.

The magnetic field becomes strongly nonlinear near the outer boundary because the return displacement current suppresses the external field.

The electric field can become increasingly nonlinear as electromagnetic energy density rises.

The relative radial gradients of these fields then modify the Maxwell stress distribution and may change the radial electromagnetic tendency from contraction to expansion.

A saturated radius $R_0$ corresponds to the approximate balance between these tendencies.

This mechanism provides the basis for the next chapter, which examines what happens when two saturated electromagnetic-wave structures overlap and whether prolonged oversaturation can cause them to reorganize into a single wider structure. [1], [2]

# 4. Merging of Electromagnetic Wave Structures

The preceding chapter introduced a simplified mechanism of radial saturation. A saturated electromagnetic wave is characterized by a transverse radius $R_0$ and approximately stable field amplitudes $E_0$ and $B_0$.

The present chapter considers what may happen when two such electromagnetic-wave structures overlap.

Because Maxwell's equations are linear in vacuum, the fields of separate electromagnetic waves may superpose without requiring a permanent interaction. In most encounters, the overlap is expected to remain temporary and the waves continue along their original propagation directions.

The present model investigates whether a different outcome may occur when two compatible electromagnetic-wave structures overlap for a sufficiently long time.

### 4.1. Temporary Superposition

Consider two electromagnetic-wave structures with fields

$$\vec{E} = \overrightarrow{E_1} + \overrightarrow{E_2}$$

and

$$\vec{B} = \overrightarrow{B_1} + \overrightarrow{B_2}$$

During overlap, the total electromagnetic energy density is

$$u = \frac{\varepsilon_0}{2}\left|\overrightarrow{E_1} + \overrightarrow{E_2}\right|^2 + \frac{1}{2\mu_0}\left|\overrightarrow{B_1} + \overrightarrow{B_2}\right|^2$$

The expansion contains the individual contributions together with cross terms.

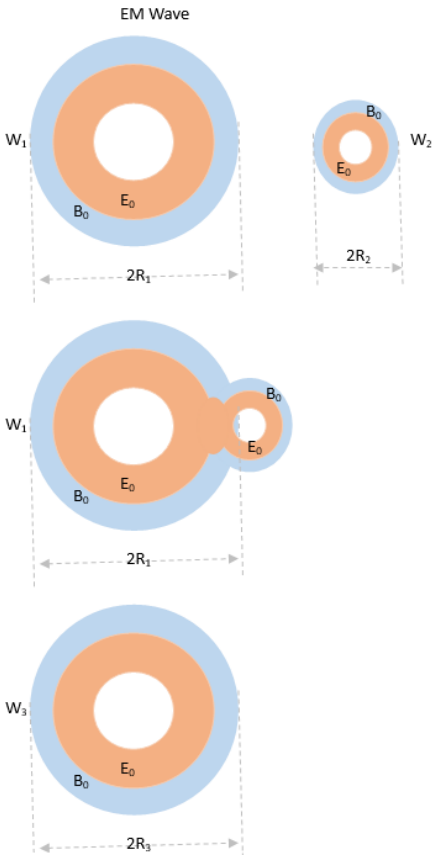


***Figure 2**. Schematic merging of two saturated electromagnetic-wave structures. Two initially separate structures with different transverse radii approach and overlap. During prolonged constructive overlap, the common region may become temporarily oversaturated and expand. If the reorganization reaches a stable state, the model proposes formation of a single wider saturated electromagnetic-wave structure. The drawing is schematic and does not represent a calculated Maxwell solution.*

For the electric field,

$$\left|\overrightarrow{E_1} + \overrightarrow{E_2}\right|^2 = E_1^2 + E_2^2 + 2\overrightarrow{E_1} \cdot \overrightarrow{E_2}$$

and similarly for the magnetic field.

The cross terms produce interference.

If the waves overlap only briefly, the resulting electromagnetic distribution exists only during the encounter. After the structures separate, each wave may continue with approximately its

original energy, radius, and propagation direction.

The model therefore distinguishes temporary interference from permanent structural merging.

**4.2. Conditions Favoring Strong Overlap**

The interaction becomes more significant when the waves possess similar electromagnetic characteristics.

The most favorable conditions include similar wavelength,

$$\lambda_1 \approx \lambda_2$$

similar frequency,

$$f_1 \approx f_2$$

similar polarization, a small phase difference,

$$|\Delta\phi| \ll \pi$$

and a small angle between the propagation directions,

$$\theta \ll 1$$

The final condition is especially important because it determines how long the transverse structures remain in contact.

For two nearly parallel waves, the relative transverse velocity is approximately

$$v_\perp \approx c$$

for small θ.

If the characteristic transverse radius is $R_0$, the corresponding overlap time is approximately

$$t_{\text{overlap}} \sim \frac{2R_0}{c\theta}$$

The overlap time therefore becomes very large as

$$\theta \to 0$$

This provides a natural distinction between rapid encounters and prolonged electromagnetic contact.

**4.3. Interference and Local Oversaturation**

Suppose two saturated waves possess approximately equal characteristic amplitudes,

$$E_1 \approx E_2 \approx E_0$$

and

$$B_1 \approx B_2 \approx B_0$$

In a region of constructive interference, the local total fields may approach

$$E_{\text{tot}} \approx 2E_0$$

and

$$B_{\text{tot}} \approx 2B_0$$

The total field therefore exceeds the characteristic saturated state of either individual wave.

Within the present model, such a region is interpreted as temporarily oversaturated.

The radial-stability mechanism described in Section 3 then predicts an outward electromagnetic tendency.

Thus, interference can provide the initial condition for transverse expansion.

**4.4. Short Encounters**

If the overlap time is short, the transverse geometry cannot change significantly before the waves separate.

Let $t_{\text{reorg}}$ denote the characteristic time required for a substantial structural response.

For

$$t_{\text{overlap}} \ll t_{\text{reorg}}$$

the waves experience only transient superposition.

The local field amplitudes may temporarily become larger or smaller through interference, but the radial geometry has insufficient time to reach a new saturated configuration.

After the encounter,

$$W_1' \approx W_1$$

$$W_2' \approx W_2$$

$$R_1' \approx R_1$$

and

$$R_2' \approx R_2$$

The structures therefore continue approximately independently.

**4.5. Prolonged Overlap**

A different situation may arise when the propagation directions are almost parallel.

If

$$t_{\text{overlap}} > t_{\text{reorg}}$$

the local oversaturation persists long enough for the transverse field profiles to adjust.

The common field region may then begin to expand.

The increasing transverse radius reduces the characteristic field amplitudes and tends to restore the saturated state.

At this stage, the configuration may still consist of two distinguishable overlapping structures.

However, if the common expanded region reaches a sufficiently developed state, the model considers the possibility that the two structures reorganize into a single electromagnetic-wave structure.

**4.6. Critical Stage of Merging**

The transition from temporary overlap to permanent merging is represented by a critical structural condition.

A simple criterion may be expressed as

$$t_{\text{overlap}} \geq t_{\text{bind}}$$

where $t_{\text{bind}}$ denotes the characteristic time required for the common field configuration to become self-sustaining.

An equivalent geometrical criterion may be introduced through a critical transverse expansion,

$$R_{\text{common}} \geq R_{\text{crit}}$$

The exact values of $t_{\text{bind}}$ and $R_{\text{crit}}$ are not yet known.

Their purpose is to distinguish two regimes.

Below the critical condition, the waves separate again.

Above it, the common electromagnetic structure becomes sufficiently developed that the original transverse boundaries are no longer restored independently.

This condition defines merging within the present model.

**4.7. Energy Conservation During Merging**

When two compatible electromagnetic-wave structures overlap for a sufficiently long time, the present model proposes that their electromagnetic fields may reorganize into a single coherent structure.

The merging process is assumed to preserve the total electromagnetic energy, provided that no energy is transferred to the surroundings or carried away by additional radiation.

All energies and propagation velocities must be defined in the same observation frame. Let (K) denote the reference frame in which the merging process is described.

For two incoming electromagnetic waves with energies $W_1^{(K)}$ and $W_2^{(K)}$, the energy of the resulting structure is

$$W_{12}^{(K)} = W_1^{(K)} + W_2^{(K)}.$$

The merging process therefore does not create additional electromagnetic energy. It redistributes the energy of the original waves into a new common electromagnetic configuration.

Within the proposed model, the electromagnetic energy of a wave may depend on the observation frame. Consequently, energies measured in different reference

frames must not be combined directly. The conservation condition must always be evaluated using quantities defined in the same frame.

During the transition, the electric and magnetic field distributions may undergo a temporary reorganization. Local field amplitudes, transverse dimensions, and the internal distribution of electromagnetic energy may change as the resulting structure approaches a new saturated state.

If the characteristic saturated field amplitudes remain approximately unchanged, the increased total energy is expected to be accommodated predominantly by an increase in the transverse dimensions of the coherent structure.

The relationship between electromagnetic energy and the saturated transverse radius is developed in Section 5.

Thus, energy conservation determines the total energy of the merged structure, while its final geometry and propagation characteristics depend on the electromagnetic reorganization occurring during merging.

### 4.8. Frequency and Propagation-Velocity Adjustment During Merging

The proposed merging mechanism requires the incoming electromagnetic waves to be sufficiently similar in their spatial field distributions.

The most favorable conditions include nearly equal wavelengths, compatible polarization, a small phase difference, and practically parallel propagation directions.

Exact equality of frequencies is not required. Two waves may possess nearly identical spatial structures while exhibiting different temporal oscillation frequencies in the selected observation frame.

The difference in frequency causes their relative phase to evolve with time. Therefore, successful merging requires that the electromagnetic reorganization occur while sufficient phase compatibility is maintained.

During the merging process, the initially separate electromagnetic fields are assumed to adjust toward a common oscillatory state.

Consider two waves described in the same observation frame K, with energies $W_1^{(K)}$ and $W_2^{(K)}$, propagation velocities $v_1^{(K)}$ and $v_2^{(K)}$, and approximately equal wavelengths:

$$\lambda_1^{(K)} \approx \lambda_2^{(K)} \approx \lambda.$$

The present model proposes, as a working hypothesis, that the resulting common propagation velocity is determined by the energy-weighted arithmetic mean of the incoming velocities:

$$v_{12}^{(K)} = \frac{W_1^{(K)} v_1^{(K)} + W_2^{(K)} v_2^{(K)}}{W_1^{(K)} + W_2^{(K)}}.$$

This relation represents a proposed dynamical property of structural merging. It is not derived from energy conservation alone.

If the resulting structure approximately preserves the common wavelength, and its propagation velocity is related to its oscillation frequency through $v = f\lambda$, the corresponding frequency becomes

$$f_{12}^{(K)} = \frac{W_1^{(K)} f_1^{(K)} + W_2^{(K)} f_2^{(K)}}{W_1^{(K)} + W_2^{(K)}}.$$

The resulting frequency therefore lies between the two incoming frequencies. For equal incoming energies, it becomes their arithmetic mean. For unequal energies, the resulting frequency is closer to that of the more energetic wave.

As an illustrative case, consider an observation frame in which the incoming propagation velocities are

$$v_1 = c + u_1, \qquad v_2 = c - u_2.$$

The proposed adjustment rule gives

$$c + \frac{W_1 u_1 - W_2 u_2}{W_1 + W_2},$$

where both energies are measured in the same observation frame.

For equal energies and equal velocity deviations in opposite directions, the resulting propagation velocity is c.

The proposed frequency and velocity adjustment is associated with the transient reorganization of the electric and magnetic fields. The detailed field dynamics, the characteristic adjustment time, and the quantitative relationship between propagation velocity and electromagnetic momentum remain to be established.

Although individual electromagnetic momentum contributions may change during interaction, the total momentum of a closed system must remain conserved. A complete momentum balance is therefore a necessary condition for a future self-consistent description of the merging process.

The present treatment does not attempt to calculate the internal forces or momentum redistribution during this transition. Its purpose is to formulate a testable relationship between incoming energies, propagation velocities, and the resulting common electromagnetic structure.

Accordingly, the energy-weighted adjustment law is retained as an explicit hypothesis of the proposed model rather than as an established consequence of linear Maxwell theory.

### 4.9. Relation Between Interference and Merging

Interference and merging are related but fundamentally different processes.

Interference begins whenever coherent electromagnetic fields overlap.

Within linear Maxwell theory, the overlapping fields superpose while the original waves remain valid independent solutions. After the overlap region ends, the waves continue propagating independently.

The present model introduces an additional possibility when constructive overlap persists for sufficiently long time.

The proposed sequence is

$$\begin{aligned}\text{overlap} &\rightarrow \text{interference}\\ &\rightarrow \text{local oversaturation}\\ &\rightarrow \text{radial expansion}\\ &\rightarrow \text{possible merging}\end{aligned}$$

The first two stages follow directly from field superposition.

The transition from oversaturation to permanent structural merging is an additional hypothesis of the present model.

If

$$t_{\text{overlap}} < t_{\text{bind}}$$

the field structure does not have sufficient time to reorganize and the waves separate again.

If

$$t_{\text{overlap}} \gtrsim t_{\text{bind}}$$

the common oversaturated region may expand sufficiently for the original transverse boundaries to cease being restored independently.

The result may then be a single common electromagnetic-wave structure.

Thus, interference is necessary for the proposed merging mechanism, but interference alone does not imply merging.

### 4.10. Experimental Consequences

The distinction between temporary overlap and structural merging makes the model experimentally testable.

The proposed transition should depend on several parameters, including wavelength, relative phase, polarization, transverse radius, crossing angle, and overlap length.

A particularly important parameter is the convergence angle

$$\theta$$

For two nearly parallel structures, the characteristic overlap time is approximately

$$t_{\text{overlap}} \sim \frac{2R_0}{c\theta}$$

A critical condition may therefore be introduced by

$$t_{\text{overlap}} \approx t_{\text{bind}}$$

which gives the approximate critical angle

$$\theta_c \sim \frac{2R_0}{ct_{\text{bind}}}$$

For

$$\theta > \theta_c$$

the overlap is expected to remain too short for substantial structural reorganization.

For

$$\theta < \theta_c$$

the common field region may persist long enough for merging to become possible.

The precise value of $\theta_c$ cannot yet be calculated because the characteristic binding time and complete three-dimensional field dynamics remain unknown.

Nevertheless, the existence of a reproducible critical angle would provide a direct experimental test of the proposed mechanism.

A decisive measurement should distinguish between ordinary interference within the overlap region and a persistent change in the outgoing electromagnetic structure after the interaction.

The following chapter therefore leaves the merging mechanism itself and considers its principal geometrical consequence: how the transverse radius changes when electromagnetic energy is incorporated into a saturated structure. [3], [4], [7]

# 5. Growth of Transverse Radius

The preceding chapter introduced the possibility that two compatible electromagnetic-wave structures may merge into a single wider structure when their overlap persists long enough for the common field configuration to reorganize.

The present chapter focuses on the geometrical consequence of this process: the increase of transverse radius as electromagnetic energy accumulates within a saturated wave structure.

### 5.1. Energy and Saturated Radius

For a saturated electromagnetic-wave structure with approximately constant characteristic field amplitudes, Part B1 introduced the approximate relation

$$W = C\lambda\varepsilon_0 E_0^2 R^2$$

where C represents the effective geometrical factor of the complete field distribution.

At fixed wavelength and comparable field geometry, this gives

$$R \propto \sqrt{W}$$

The transverse radius therefore increases as the square root of the energy contained in the electromagnetic-wave structure.

The model does not require the characteristic field amplitudes to increase permanently as more energy is added. Instead, the additional energy may be accommodated by enlarging the transverse region occupied by the saturated fields.

### 5.2. Addition of Energy to a Saturated Structure

Consider an initially saturated electromagnetic wave with energy $W_1$ and radius $R_1$.

If additional energy $\Delta W$ is incorporated into the same structure, the new energy is

$$W_2 = W_1 + \Delta W$$

If the final state returns to the same characteristic saturated amplitudes, then

$$R_2 = R_{1\sqrt{\frac{W_2}{W_1}}}$$

or equivalently

$$R_2 = R_{1\sqrt{1+\frac{\Delta W}{W_1}}}$$

This relation shows that the effect of a given added energy depends on the size of the initial structure.

A small saturated wave can increase its radius substantially when it receives an energy comparable to its own.

A large wave receiving the same absolute amount of energy changes its radius only slightly.

**5.3. Equal-Wave Merging**

For two equal saturated waves,

$$W_1 = W_2 = W$$

and

$$R_1 = R_2 = R_0$$

the merged energy is

$$W_3 = 2W$$

and the resulting radius is

$$R_3 = \sqrt{2}R_0$$

The energy therefore doubles, while the radius increases only by the factor

$$\sqrt{2} \approx 1.414$$

This is a direct consequence of the approximate quadratic dependence of energy on transverse radius.

Repeated merging produces progressively larger structures, but the radius grows more slowly than the total energy.

**5.4. Repeated Accumulation of Equal Structures**

Suppose a sequence of N equal saturated electromagnetic-wave structures merges into one common structure.

The total energy becomes

$$W_N = NW_0$$

while the transverse radius becomes

$$R_N = \sqrt{N}R_0$$

Thus, increasing the radius by a factor of ten requires approximately one hundred times the initial energy:

$$R_N = 10R_0 \Rightarrow W_N = 100W_0$$

The growth of a wide electromagnetic-wave structure therefore requires the accumulation of many smaller energy contributions.

**5.5. Merging of Unequal Structures**

Consider two saturated waves with different transverse radii.

Their energies satisfy approximately

$$\frac{W_2}{W_1} = \frac{R_2^2}{R_1^2}$$

for the same wavelength and comparable geometry.

After complete merging,

$$R_3 = \sqrt{R_1^2 + R_2^2}$$

If

$$R_2 \gg R_1$$

then the resulting radius may be written approximately as

$$R_3 \approx R_2\left(1 + \frac{R_1^2}{2R_2^2}\right)$$

A small electromagnetic wave can therefore contribute its entire energy to a much larger structure while causing only a small fractional increase in its radius.

This illustrates why large energy differences between saturated waves do not require

correspondingly large differences in their local characteristic field amplitudes.

**5.6. Temporary Oversaturation During Growth**

The increase of radius is not assumed to occur instantaneously.

When additional electromagnetic energy first enters a saturated structure, its transverse geometry initially remains approximately unchanged.

The characteristic field amplitudes therefore rise above their saturated values.

The structure becomes temporarily oversaturated.

The radial mechanism developed in Section 3 then produces an outward tendency.

As the radius increases, the energy is distributed over a larger transverse region and the field amplitudes decrease toward their saturated values.

The growth process may therefore be represented schematically as

$$W \uparrow \Rightarrow E, B > E_0, B_0 \Rightarrow \text{oversaturation} \Rightarrow R \uparrow \Rightarrow E, B \rightarrow E_0, B_0$$

The final state is a wider saturated electromagnetic-wave structure containing more total energy.

**5.7. Growth by Successive Encounters**

A propagating electromagnetic wave may encounter compatible structures at different positions along its trajectory.

Each successful merging event may increase its energy and transverse radius.

If the accumulated structure subsequently encounters additional waves under favorable conditions, the process can continue.

The model therefore permits a sequence

$$R_1 < R_2 < R_3 <$$

accompanied by

$$W_1 < W_2 < W_3 <$$

while the characteristic saturated field amplitudes remain approximately unchanged.

The resulting electromagnetic wave can therefore become progressively wider and more energy-rich during propagation.

**5.8. Conservation of Energy**

The increase in transverse radius does not create energy.

For every merging event, the total energy of the resulting structure must equal the energy initially contained in the participating electromagnetic waves, apart from any energy radiated or transferred elsewhere.

The idealized condition is

$$W_{\text{final}} = \sum_i W_i$$

The geometrical growth of the wave is therefore interpreted as a redistribution of conserved electromagnetic energy into a larger saturated field volume.

**5.9. Transverse Growth and Field Amplitude**

The distinction between total energy and local field amplitude is central to the proposed model.

A larger electromagnetic-wave structure may contain far more total energy than a smaller one even when both possess the same characteristic saturated amplitudes.

Thus,

$$E_1 \approx E_2 \approx E_0$$

and

$$B_1 \approx B_2 \approx B_0$$

do not imply

$$W_1 = W_2$$

because the transverse geometries may be very different.

The energy difference can instead be represented through the transverse radii.

For comparable saturated structures,

$$\frac{W_2}{W_1} \approx \left(\frac{R_2}{R_1}\right)^2$$

This provides a geometrical interpretation of energy accumulation within the proposed electromagnetic-wave model.

### 5.10. Experimental Significance

The relationship between energy and transverse radius provides a direct connection between the proposed merging mechanism and experimental measurement.

If larger electromagnetic-wave energies correspond to larger transverse radii, then measurements capable of constraining the transverse extent of the wave may also provide indirect information about the structural accumulation of electromagnetic energy.

The double-slit experiment is particularly useful because the slit separation can be varied over a known transverse distance.

If a maximum effective separation exists beyond which the wave can no longer contribute coherently to both apertures, this distance may constrain the transverse radius of the electromagnetic structure.

The next chapter therefore examines how a double-slit arrangement may be used to estimate the characteristic transverse dimension $R_0$. [1], [7], [8]

## 6. Measurement of the Transverse Radius $R_0$

The preceding chapters introduced the transverse radius $R_0$ as a characteristic dimension of a saturated electromagnetic-wave structure.

If this radius represents a real physical dimension of the electromagnetic field, it should in principle be measurable.

The double-slit experiment provides a particularly simple geometry for investigating this possibility because the separation between the two apertures can be varied while the wavelength, slit width, source, and observation geometry are controlled.

The present chapter examines how such measurements may constrain the transverse extent of the proposed electromagnetic-wave structure.

### 6.1. Double-Slit Geometry

Consider two narrow slits separated by a center-to-center distance d.

An electromagnetic-wave structure approaching the double slit may intersect both apertures if its transverse field distribution extends over the required distance.

For a wave whose axis passes approximately midway between the slits, the transverse distance from the axis to either slit is

$$\frac{d}{2}$$

If the electromagnetic field becomes negligible outside the effective transverse radius $R_{\mathrm{det}}$, simultaneous significant coupling to both slits requires approximately

$$\frac{d}{2} \lesssim R_{\mathrm{det}}$$

or

$$d \lesssim 2R_{\mathrm{det}}$$

If the experimentally relevant outer boundary lies close to the characteristic saturated radius $R_0$, this condition becomes approximately

$$d_{max} \approx 2R_0$$

The largest slit separation for which the characteristic two-slit interference remains observable may therefore provide an

experimental estimate or upper constraint on the transverse size of the electromagnetic-wave structure.

### 6.2. Characteristic Radius and Detectable Radius

The physical field boundary need not coincide exactly with the characteristic radius $R_0$.

The magnetic field may reach its characteristic maximum near $R_0$ and then decrease through the outer return-current region before becoming negligible.

It is therefore useful to distinguish the characteristic radius $R_0$ from an experimentally defined detectable radius $R_{\mathrm{det}}$.

A practical field threshold may be introduced as

$$B(R_{\mathrm{det}}) = \eta B_0$$

where η is determined by the sensitivity of the experiment.

For example, a one-percent boundary is defined by

$$B\left(R_{1\backslash\%}\right) = 0.01 B_0$$

If the outer magnetic boundary is sufficiently sharp, then

$$R_{\mathrm{det}} \approx R_0$$

to within the thickness of the outer boundary region.

The experimentally inferred value should therefore initially be regarded as an effective transverse radius rather than an exact geometrical boundary.

### 6.3. Random Position of the Incoming Wave

The axis of an individual electromagnetic-wave structure need not pass through the midpoint between the slits.

The wave may arrive at any transverse position.

If its center is displaced by a distance $x_0$, the distances to the two slits are approximately

$$r_1 = \left| x_0 - \frac{d}{2} \right|$$

and

$$r_2 = \left| x_0 + \frac{d}{2} \right|$$

Both apertures can receive significant field contributions only when

$$r_1 \lesssim R_{\mathrm{det}}$$

and

$$r_2 \lesssim R_{\mathrm{det}}$$

simultaneously.

As the slit separation approaches the transverse diameter of the wave, the range of possible incoming positions satisfying both conditions becomes increasingly narrow.

Thus, even before interference disappears completely, the fraction of electromagnetic-wave structures capable of significantly illuminating both slits should decrease.

This may produce a gradual reduction in interference visibility as dd approaches the effective transverse diameter.

### 6.4. Expected Dependence on Slit Separation

If the transverse electromagnetic field has a finite outer extent, the model predicts three qualitative regimes.

For

$$d \ll 2R_{\mathrm{det}}$$

a large range of incoming transverse positions allows significant field contributions at both slits.

The interference pattern should therefore be readily formed.

As

$$d \to 2R_{\mathrm{det}}$$

only increasingly favorable transverse positions contribute significantly to both slits.

The visibility or statistical strength of the interference pattern may consequently decrease.

For

$$d > 2R_{\mathrm{det}}$$

a single sharply bounded electromagnetic-wave structure cannot simultaneously extend over both slit centers in the simplified geometrical picture.

The model therefore predicts that a characteristic change in the interference behavior should occur near this transverse scale.

**6.5. Distinction from Ordinary Beam Width**

An important experimental distinction must be made between the proposed radius $R_0$ of an individual electromagnetic-wave structure and the macroscopic width of the illuminating beam.

A laser beam may have a transverse diameter of millimeters or centimeters and contain many electromagnetic contributions.

The fact that the complete beam illuminates both slits does not by itself establish that an individual proposed wave structure has the same transverse radius.

Therefore, measurements intended to constrain $R_0$ must control the transverse illumination as carefully as possible.

The width and intensity profile of the incoming beam should be measured independently.

The experiment should then determine whether the disappearance or reduction of interference follows the macroscopic beam profile or reveals an additional characteristic transverse scale.

**6.6. Interference Visibility as a Measurement Quantity**

A useful experimental quantity is the fringe visibility

$$V = \frac{I_{max} - I_{min}}{I_{max} + I_{min}}$$

where $I_{max}$ and $I_{min}$ are neighboring maximum and minimum intensities.

Rather than defining a sharp boundary through the complete disappearance of the interference pattern, the experiment may measure

$$V = V(d)$$

while the slit separation is systematically varied.

The proposed electromagnetic-wave model suggests that a characteristic reduction may occur as the separation approaches the effective transverse diameter.

The experimentally defined maximum useful separation may then be specified by a chosen threshold visibility $V_{min}$:

$$V(d_{max}) = V_{min}$$

The corresponding effective radius would be

$$R_{\mathrm{det}} \approx \frac{d_{max}}{2}$$

within the simplified symmetric geometry.

**6.7. Dependence on Wavelength**

The measurement should be repeated for several wavelengths.

Part B1 does not assume a universal proportionality between the longitudinal wavelength and the transverse radius.

Therefore, the experiment should not impose in advance a relation of the form

$$R_0 \propto$$

Instead, $R_0$ should be determined independently for each wavelength and energy condition.

Measurements at different wavelengths may reveal whether the transverse radius is primarily related to wavelength, total wave

energy, saturation conditions, or another structural parameter.

This distinction is particularly important because the model associates the transverse radius with electromagnetic energy as well as with field geometry.

### 6.8. Dependence on Electromagnetic-Wave Energy

For saturated structures with similar geometry, the proposed energy relation is

$$W = C\lambda\varepsilon_0 E_0^2 R_0^2$$

Thus, at fixed wavelength and approximately constant saturated amplitude,

$$R_0 \propto \sqrt{W}$$

If electromagnetic-wave structures of different energies can be prepared while maintaining comparable wavelength and field state, the model predicts different transverse radii.

A measurement of the maximum effective slit separation may therefore also be performed as a function of wave energy.

The predicted qualitative trend is

$$W \uparrow \Rightarrow R_0 \uparrow \Rightarrow d_{max}$$

A reproducible dependence of the inferred transverse scale on energy would provide an important test of the proposed model.

### 6.9. Comparison with Conventional Diffraction and Coherence

The existence of an interference pattern depends on more than the transverse extent of the proposed electromagnetic-wave structure.

Standard optical effects must also be taken into account, including slit diffraction, spatial coherence, temporal coherence, finite source size, polarization, spectral width, and detector sensitivity.

In conventional wave optics, interference can remain observable for large slit separations if the illumination remains sufficiently coherent and the diffracted fields from both apertures overlap at the detector.

Therefore, the observation of interference at a particular slit separation does not by itself determine $R_0$.

The appropriate comparison is therefore not simply between interference and no interference, but between the measured dependence

$$V_{\mathrm{meas}}(d)$$

and the dependence expected from conventional diffraction and coherence theory,

$$V_{\mathrm{conv}}(d)$$

A systematic additional reduction associated with a reproducible transverse scale would be of particular interest.

### 6.10. Experimental Procedure

A suitable measurement could proceed in the following sequence.

A narrow-band coherent source is directed toward a double-slit system with accurately known slit width and adjustable slit separation.

The wavelength and polarization are held fixed.

The observation distance is chosen sufficiently large that the diffracted contributions from both slits overlap clearly.

For each slit separation, the complete intensity pattern is recorded and the fringe visibility is determined.

The slit separation is then progressively increased.

The procedure is repeated for several observation distances in order to separate transverse-size effects from the geometric development of Fresnel and Fraunhofer diffraction.

It should also be repeated for different source powers and wavelengths.

The resulting data provide

$$V = V(d, L, \lambda, W)$$

From these measurements one may determine whether an additional characteristic transverse scale is present.

**6.11. Measurement of the Outer Boundary**

If a finite transverse field boundary exists, the decrease in interference visibility may contain information not only about $R_0$ but also about the sharpness of the outer boundary.

A very sharp field boundary would tend to produce a relatively rapid change as d approaches the effective transverse diameter.

A broad outer field tail would instead produce a more gradual decrease.

Thus, the measured function V(d) may potentially constrain both the characteristic radius and the boundary thickness.

The experiment may therefore provide information about

$$R_0$$

and

$$\Delta R = R_{\text{out}} - R_0$$

rather than only one transverse dimension.

**6.12. Interpretation of the Measurement**

Within the proposed model, a measured maximum effective slit separation would not imply that the field terminates mathematically at exactly one radius.

It would define the transverse distance over which the electromagnetic field remains sufficiently strong and coherent to contribute measurably to both apertures.

Thus, the relation

$$R_0 \approx \frac{d_{max}}{2}$$

should initially be regarded as an operational estimate.

A more precise determination requires the radial field profile obtained from the boundary model developed in Section 2.

The measurement of $R_0$ therefore connects directly with the theoretical description of the outer electromagnetic boundary.

**6.13. Experimental Significance**

A reproducible finite transverse scale would be one of the most direct tests of the proposed electromagnetic-wave structure.

If a characteristic separation appears consistently after conventional effects are accounted for, it could provide an empirical constraint on the transverse dimensions of the electromagnetic wave.

The double-slit experiment may therefore serve not only as a demonstration of interference but also as a quantitative test of the proposed three-dimensional field geometry.

The next chapter examines a second use of the same geometry: determining the convergence angle and overlap conditions under which separate electromagnetic-wave structures may begin to merge. [3], [4], [5]

# 7. Measurement of the Critical Convergence Angle

The preceding chapter considered the double-slit experiment as a possible method for constraining the transverse radius of an electromagnetic-wave structure. The same experimental geometry can also be used to investigate a second quantity: the angle at which two electromagnetic-wave structures overlap long enough to undergo structural reorganization.

The present model distinguishes ordinary interference from permanent merging. Interference begins whenever compatible electromagnetic fields overlap. Merging, however, is assumed to require sufficiently

favorable wavelength, phase, polarization, propagation direction, and overlap time.

The convergence angle therefore becomes an experimentally relevant parameter.

### 7.1. Geometrical Definition of the Convergence Angle

Consider two contributions emerging from two slits separated by a distance d. Let the corresponding electromagnetic-wave structures overlap at a point located approximately a distance L from the slit plane.

For symmetric geometry, the angle between the two propagation directions is

$$\theta = 2\arctan\left(\frac{d}{2L}\right)$$

For small angles,

$$\theta \approx \frac{d}{L}$$

Thus, increasing the observation distance reduces the angle between the two converging contributions.

This provides a simple geometrical method for controlling the overlap angle experimentally.

### 7.2. Overlap Time

For two electromagnetic-wave structures of characteristic transverse radius $R_0$, the overlap time depends strongly on their relative angle.

For small θ, the relative transverse velocity is approximately

$$v_\perp \approx c$$

The characteristic time during which the two transverse structures remain significantly overlapped may therefore be estimated as

$$t_{\text{overlap}} \sim \frac{2R_0}{c\theta}$$

Substituting the small-angle double-slit approximation gives

$$t_{\text{overlap}} \sim \frac{2R_0 L}{cd}$$

The overlap time therefore increases with observation distance and decreases with slit separation.

This relation provides a direct connection between measurable geometrical quantities and the proposed structural interaction time.

### 7.3. Critical Overlap Condition

The merging model introduced a characteristic binding or reorganization time $t_{\text{bind}}$.

Temporary interference is expected when

$$t_{\text{overlap}} < t_{\text{bind}}$$

whereas structural merging may become possible when

$$t_{\text{overlap}} \geq t_{\text{bind}}$$

The corresponding critical angle is approximately

$$\theta_c \sim \frac{2R_0}{ct_{\text{bind}}}$$

For

$$\theta > \theta_c$$

the overlap is too brief for substantial radial reorganization.

For

$$\theta < \theta_c$$

the fields remain overlapped long enough for the common oversaturated region to develop.

The exact value of $\theta_c$ is not derived in the present model and must therefore be determined experimentally.

### 7.4. Critical Observation Distance

The convergence-angle condition can be expressed in terms of the observation distance.

From

$$\theta_c = 2\arctan\left(\frac{d}{2L_c}\right)$$

the critical distance is

$$L_c = \frac{d}{2\tan(\theta_c/2)}$$

For small critical angles,

$$L_c \approx \frac{d}{\theta_c}$$

This gives a simple experimental prediction.

If a characteristic merging angle exists, then the critical distance should scale approximately linearly with slit separation:

$$L_c \propto d$$

provided the wavelength, polarization, phase conditions, and electromagnetic-wave radius remain comparable.

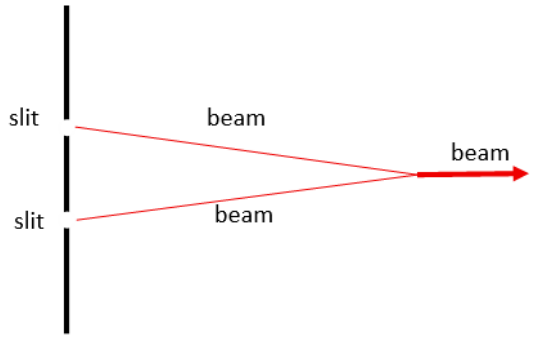


**Figure 3.** *Double-slit geometry for studying the transverse extent and convergence of electromagnetic-wave structures. Electromagnetic contributions emerging from two slits separated by distance d approach one another and overlap at a distance L. The geometry can be used to investigate both the effective transverse radius and the convergence angle associated with prolonged coupling.*

This proportionality provides a useful experimental test because it separates an angular criterion from a fixed-distance effect.

### 7.5. Development of the Interference Pattern

At short observation distances, the angle between the contributions from the two slits is relatively large.

The electromagnetic-wave structures may still interfere during their brief overlap, but the overlap time may be insufficient for significant transverse reorganization.

As the observation distance increases, the angle decreases and the overlap length increases.

The model therefore predicts a possible sequence

large angle → short overlap
→ temporary interference

followed by

small angle → long overlap
→ possible merging

The resulting intensity pattern may therefore contain information about the transition from transient interference to structural coupling.

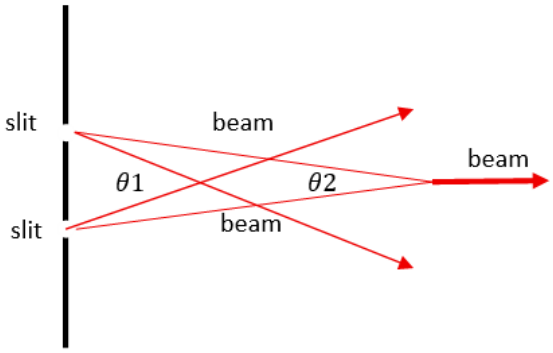


**Figure 4.** *<u>Geometrical interpretation of the critical convergence angle.</u> Electromagnetic-wave contributions emerging from the two slits propagate along different directions and overlap downstream. The angles $(\theta_1)$ and $(\theta_2)$ describe the convergence of the two wave structures toward the common overlap region. For sufficiently small convergence angles, the overlap length and overlap time increase. Within the proposed model, prolonged constructive overlap may allow the initially separate structures to reorganize into a common electromagnetic-wave structure. The transition from independent propagation to possible structural coupling is therefore expected to depend on the convergence geometry and on the total overlap time.*

### 7.6. Experimental Search for a Critical Angle

A practical experiment may use a double-slit system with adjustable slit separation.

For a fixed wavelength and source condition, the observation distance is varied systematically.

At each distance, the complete interference pattern is recorded and its visibility determined.

The same procedure is then repeated for several slit separations.

For every d, one may identify a characteristic distance $L_c$ at which an additional change in the interference behavior becomes apparent.

The corresponding angle is calculated from

$$\theta_c = 2\arctan\left(\frac{d}{2L_c}\right)$$

If the model is correct, measurements performed with different slit separations should yield approximately the same critical angle under comparable electromagnetic conditions.

Thus,

$$\theta_c(d_1) \approx \theta_c(d_2) \approx \theta_c(d_3)$$

would be a particularly interesting result.

### 7.7. Dependence on Wavelength

The critical convergence angle may depend on wavelength.

The transverse field structure, overlap length, and reorganization time may all change with λ.

Therefore, the experiment should be repeated for several wavelengths.

The measured function

$$\theta_c = \theta_c(\lambda)$$

would provide information about the relationship between longitudinal periodicity and transverse coupling.

The model does not assume in advance that $\theta_c$ is independent of wavelength.

### 7.8. Dependence on Transverse Radius

From the approximate overlap-time relation,

$$t_{\text{overlap}} \sim \frac{2R_0}{c\theta}$$

a larger transverse radius increases the duration of overlap at the same angle.

Thus, if the binding time remains comparable, larger electromagnetic-wave structures may merge at somewhat larger angles.

The critical angle may therefore depend on transverse radius approximately as

$$\theta_c \propto R_0$$

for fixed $t_{\text{bind}}$.

Because $R_0$ itself may depend on electromagnetic-wave energy, the convergence measurement may also reveal an indirect energy dependence.

### 7.9. Dependence on Relative Phase

The overlap angle alone is not sufficient to determine whether merging occurs.

The local electromagnetic field depends strongly on the relative phase.

For nearly equal waves, the local field amplitude depends on the phase difference according to

$$E_{\text{tot}} = 2E_0\cos\left(\frac{\Delta\phi}{2}\right)$$

for equal amplitudes at a selected point.

Constructive interference,

$$\Delta\phi \approx 0$$

produces the strongest local oversaturation.

For

$$\Delta\phi \approx \pi$$

the local electric field can instead become strongly reduced.

The model therefore predicts that structural merging should be most favorable when the relative phase produces sustained constructive overlap.

**7.10. Dependence on Polarization**

The vector orientation of the fields is also important.

Parallel polarizations allow strong constructive and destructive interference.

Orthogonal polarizations do not produce the same local amplitude modulation.

Therefore, the merging probability should depend on relative polarization.

A controlled polarization experiment can provide an additional test.

For parallel polarization,

$$\overrightarrow{E_1} \parallel \overrightarrow{E_2}$$

strong local oversaturation is possible.

For orthogonal polarization,

$$\overrightarrow{E_1} \perp \overrightarrow{E_2}$$

the field combination is qualitatively different.

A strong dependence of the proposed coupling threshold on polarization would therefore be expected.

**7.11. Critical Angle as a Structural Parameter**

If a reproducible critical angle is found after conventional diffraction and coherence effects are accounted for, it would represent a new experimentally defined parameter of the proposed electromagnetic-wave structure.

Together with the transverse radius $R_0$, it would constrain the characteristic reorganization time.

From

$$t_{\text{bind}} \sim \frac{2R_0}{c\theta_c}$$

measurement of $R_0$ and θc would provide an estimate of the time required for the overlapping fields to develop a common structure.

The double-slit experiment could therefore provide two independent pieces of structural information:

$$d_{max} \rightarrow \backslash R_0$$

and

$$\frac{d}{L_c} \rightarrow \theta_c$$

The first concerns the transverse extent of the electromagnetic wave.

The second concerns the dynamics of electromagnetic-wave coupling.

**7.12. Experimental Significance**

The measurement of a critical convergence angle offers a direct way to test the proposed distinction between temporary interference and permanent structural merging.

If all observed changes with angle and distance are fully described by conventional diffraction and coherence theory, no additional coupling mechanism is required.

If, however, a reproducible transition appears at a characteristic convergence angle and remains consistent across different slit separations, it would provide evidence for an additional structural process.

The combination of transverse-radius measurements and convergence-angle measurements therefore offers a practical experimental route for examining the proposed geometry and dynamics of electromagnetic-wave structures. [4], [6], [7]

## 8. Evolution of EM-Wave Energy and Transverse Size During Propagation

The electromagnetic wave described in the present model should not be regarded as a structure whose energy and transverse dimensions necessarily remain unchanged from emission to detection. During propagation, the wave can interact with other electromagnetic waves, with matter, and with external fields. Its total energy W and characteristic transverse radius $R_0$ can therefore evolve along the propagation path.

A particularly important process is coherent merging.

Electromagnetic waves emitted by the same source commonly propagate in approximately the same direction. Their mutual convergence angle can therefore be small,

$$\theta \approx 0$$

As discussed in the preceding sections, small convergence angles provide favorable conditions for coherent merging. Two or more initially separate electromagnetic structures can consequently reorganize into a larger coherent electromagnetic wave.

Schematically,

$$W_1 + W_2 \rightarrow W_{12}$$

If losses during the merging event are small,

$$W_{12} \approx W_1 + W_2$$

The characteristic field amplitudes $E_0$ and $B_0$ need not increase proportionally with this additional energy. In the saturation picture developed earlier, the additional energy can instead be accommodated predominantly through growth of the coherent transverse structure.

Thus,

$$W \uparrow \quad \Rightarrow \quad R_0$$

The precise relation

$$R_0 = R_0(W)$$

depends on the internal geometry and energy distribution of the electromagnetic wave and remains one of the quantitative problems of the model.

Repeated merging can therefore produce a cumulative evolution:

many small EM waves
→ fewer larger EM waves
→ large coherent EM structures

An electromagnetic wave arriving at a distant target may consequently possess an energy and transverse radius many orders of magnitude greater than those of the elementary structures initially produced near the source.

This provides a possible physical interpretation of the large transverse coherence observed in optical interference experiments. Within the present model, such coherence is interpreted as the macroscopic result of coherent organization and repeated merging of initially smaller electromagnetic-wave structures.

Propagation, however, does not produce growth only.

An electromagnetic wave can also lose energy through interactions with matter. Scattering from atoms, molecules, dust particles, droplets, or other material structures can remove energy from the coherent wave or divide the original structure into smaller independently propagating parts.

Such a process can be represented schematically as

$$W \rightarrow W - \Delta W$$

Because $R_0$ is connected with the total energy contained in the coherent structure, energy loss is accompanied by a reduction of its characteristic transverse size,

$$W \downarrow \quad \Rightarrow \quad R_0 \downarrow$$

The propagation of an electromagnetic wave can therefore be understood as a competition between two classes of processes:

$$\text{coherent\merging} \rightarrow W \uparrow, \backslash R_0 \uparrow$$

and

$$\text{energy loss or fragmentation} \rightarrow W \downarrow, \backslash R_0 \downarrow$$

The actual state of the electromagnetic wave at a detector is determined by the cumulative balance of these processes along its trajectory.

A general schematic energy balance may therefore be written as

$$\frac{dW}{ds} = G_{\text{merge}} - L_{\text{matter}} - L_{\text{other}} + G_{\text{ext}}$$

where s is distance along the propagation path, $G_{\text{merge}}$ represents energy acquired through coherent merging, $L_{\text{matter}}$ represents losses associated with interactions with matter, $L_{\text{other}}$ includes other loss or fragmentation mechanisms, and $G_{\text{ext}}$ represents energy exchange with external fields.

Since

$$R_0 = R_0(W)$$

the evolution of the transverse radius follows from the energy evolution,

$$\frac{dR_0}{ds} = \frac{dR_0}{dW}\frac{dW}{ds}$$

This formulation does not require the exact function $R_0(W)$ to be known in advance. It only requires the structural property established earlier in the model:

$$\frac{dR_0}{dW} > 0$$

**8.1. Gravitational Energy Exchange**

Part A4 assigns both momentum and an effective gravitational response to the electromagnetic structure. Within that model, propagation through a gravitational field provides another mechanism by which W and therefore $R_0$ can change.

When an electromagnetic wave propagates outward against a gravitational field, part of its energy is transferred into gravitational potential energy. Its local electromagnetic energy therefore decreases,

$$\Delta W < 0$$

and the corresponding structural response is

$$\Delta R_0 < 0$$

Thus,

$$\text{propagation against gravity} \quad \Rightarrow W \downarrow, R0 \downarrow$$

For propagation toward a gravitational source, the opposite evolution is expected within the model:

$$\text{propagation with gravity} \quad \Rightarrow \quad W \uparrow, \backslash R_0 \uparrow$$

The gravitational interaction would therefore affect not only the energy associated with the electromagnetic wave but also its transverse structural organization.

This interpretation provides a direct connection between Parts III and V. Part A4 considers the gravitational and inertial properties associated with electromagnetic structures, while the present section identifies how an exchange of energy during propagation can appear geometrically as a change in $R_0$.

**8.2. Propagation as Structural Evolution**

The electromagnetic wave reaching a detector should therefore not automatically be identified with the elementary electromagnetic structure produced at the source.

Its history may contain repeated processes of merging, fragmentation, scattering, and energy exchange with external fields.

Consequently,

$$W_{\text{det}} \neq W_{\text{source}}$$

and

$$R_{0,\text{det}} \neq R_{0,\text{source}}$$

in general.

For radiation propagating through a sufficiently clean region in which coherent merging dominates over losses, the model predicts

$$W_{\mathrm{det}} \gg W_{\mathrm{source}}$$

and

$$R_{0,\mathrm{det}} \gg R_{0,\mathrm{source}}$$

Conversely, propagation through strongly scattering or absorbing matter can reduce both quantities.

The observed electromagnetic wave is therefore the result of its **propagation history**, rather than merely a preserved copy of the structure produced at emission.

A particularly important consequence for the photoelectric interaction developed in Part B3 is that the total energy of the electromagnetic wave reaching an atom need not be limited to the locally transferred photoelectric energy. After repeated coherent merging,

$$W_{\mathrm{wave}} \gg W_{\mathrm{tr}}$$

may be possible, while at the photoelectric threshold the local transferred energy remains of the order

$$W_{\mathrm{tr}} \sim hf$$

Thus, Part B2 provides a mechanism by which large and energy-rich coherent electromagnetic waves can develop during propagation, while Part B3 describes how only a limited local part of such a structure participates in an individual electron-ejection event. [1], [3], [7]

# 9. Open Problems and Decisive Tests

The preceding chapters developed several specific consequences of the proposed electromagnetic-wave structure. These include a finite transverse extent, a return displacement-current boundary, a saturated transverse state, an energy-dependent radius, and the possible structural reorganization of sufficiently long overlapping waves.

The purpose of the present chapter is not to repeat the experimental procedures already described in Sections 6 and 7, but to identify the observations that would most clearly distinguish the proposed model from conventional electromagnetic-wave propagation and to state the principal theoretical problems that remain unresolved.

### 9.1. Finite Transverse Scale

The most direct structural prediction is the existence of a reproducible transverse scale associated with an individual electromagnetic-wave structure.

The proposed characteristic radius is

$$R_0$$

while the experimentally detectable radius is

$$R_{\mathrm{det}}$$

and the outer field boundary is represented by

$$R_{\mathrm{out}}$$

A decisive measurement would require evidence for a characteristic transverse scale that remains after conventional beam width, spatial coherence, temporal coherence, diffraction, source size, polarization, detector sensitivity, and propagation geometry have been accounted for.

The double-slit experiment can provide an initial constraint through the approximate geometrical relation

$$R_{\mathrm{det}} \approx \frac{d_{max}}{2}$$

but this relation is a prediction of the proposed finite-wave model and not a standard result of double-slit optics.

A remaining experimental difficulty is that the present model does not yet specify how a single electromagnetic-wave structure can be isolated within a macroscopic coherent beam.

Double-slit measurements should therefore initially be interpreted as constraints on a possible transverse structural scale rather than as an unambiguous direct measurement of one isolated structure.

### 9.2. Outer Boundary and Return Displacement Current

The boundary mechanism developed in Section 2 predicts that the longitudinal displacement current changes sign across the transverse section.

The essential cancellation condition is

$$\int_0^{R_{\mathrm{out}}} J_{D,z}(r)\, r\, dr = 0$$

The smooth example introduced in Section 2.5 demonstrates that such a distribution can contain an inner displacement current, an oppositely directed outer return region, and a magnetic field that approaches zero at the outer radius.

The remaining theoretical task is to embed this radial structure into a complete three-dimensional source-free Maxwell field.

A successful solution must reproduce simultaneously the sign reversal of $J_{D,z}$, the associated magnetic profile, the required transverse electric-field components, and longitudinal propagation.

Thus, the existence of a mathematically consistent smooth radial cancellation profile has been demonstrated, while its incorporation into a complete propagating field remains open.

### 9.3. Saturation and the Energy-Radius Relation

The proposed saturation mechanism predicts that electromagnetic-wave structures approach a radial state in which electric and magnetic stress contributions approximately balance.

The integrated stress condition introduced in Section 3 is

$$E_0^2 I_E = c^2 B_0^2 I_B$$

This condition shows that saturation depends on both characteristic amplitudes and radial field profiles.

For geometrically similar saturated structures, the model further proposes

$$W = C\lambda\varepsilon_0 E_0^2 R_0^2$$

and therefore, at fixed wavelength and comparable saturated field amplitudes,

$$R_0^2 \propto W$$

This is one of the clearest quantitative predictions of the model.

A decisive experimental test would determine whether increasing electromagnetic-wave energy produces systematic transverse growth while the characteristic local field amplitudes remain approximately associated with the saturated state.

The geometrical factor C remains dependent on the complete field profile and cannot yet be assigned a universal numerical value.

### 9.4. Direct Test of Structural Merging

Interference alone is not a sufficient test of the proposed merging mechanism.

Within linear Maxwell theory, overlapping waves superpose and subsequently continue as independent solutions.

The proposed model predicts an additional possibility: sufficiently prolonged constructive overlap may produce a persistent reorganization of the outgoing electromagnetic field.

The relevant condition is expressed through the ratio of overlap time to structural reorganization time.

$$t_{\mathrm{overlap}} \gtrsim t_{\mathrm{reorg}}$$

For nearly parallel wave structures,

$$t_{\mathrm{overlap}} \sim \frac{2R_0}{c\theta}$$

and a corresponding characteristic angle may be estimated as

$$\theta_c \sim \frac{2R_0}{ct_{\mathrm{reorg}}}$$

The most decisive experiment would therefore use two independently controlled coherent beams with adjustable wavelength, phase, polarization, crossing angle, and overlap length.

The decisive observable is not enhanced or reduced intensity inside the overlap region. It is a persistent change in the outgoing field that cannot be represented as the original two waves continuing independently through one another.

**9.5. Momentum Conservation**

Any proposed merging process must satisfy both energy and momentum conservation.

For a freely propagating electromagnetic wave,

$$p = \frac{W}{c}$$

For two equal waves of energy $W$ meeting at an angle $\theta$, the magnitude of their total momentum is

$$p_{\mathrm{tot}} = \frac{2W}{c}\cos\left(\frac{\theta}{2}\right)$$

while their total energy is

$$W_{\mathrm{tot}} = 2W$$

For any finite crossing angle,

$$p_{\mathrm{tot}} < \frac{W_{\mathrm{tot}}}{c}$$

Therefore, two non-collinear waves cannot in general reorganize into one ordinary freely propagating wave containing the complete initial energy without an additional redistribution of energy and momentum.

Possible mechanisms may include internal transverse momentum, additional field structure, or radiation during reorganization.

The limit

$$\theta \to 0$$

minimizes this difficulty and is therefore the most favorable regime for experimental searches for structural merging.

This momentum condition is not merely a secondary detail. It is a fundamental constraint that any complete merging model must satisfy.

**9.6. Complete Maxwell and Momentum Solution**

The principal theoretical problem is the construction of a self-consistent three-dimensional electromagnetic solution.

Such a solution must simultaneously reproduce:

- finite transverse field concentration,
- inner and return displacement-current regions,
- suppression of the external magnetic field,
- compatible longitudinal and transverse electric-field components,
- periodic longitudinal propagation,
- electromagnetic energy continuity,
- radial stress balance,
- and electromagnetic momentum conservation.

The fields must satisfy the source-free Maxwell equations,

$$\nabla \cdot \vec{E} = 0$$

$$\nabla \cdot \vec{B} = 0$$

$$\nabla \times \vec{E} = -\frac{\partial \vec{B}}{\partial t}$$

$$\nabla \times \vec{B} = \mu_0 \varepsilon_0 \frac{\partial \vec{E}}{\partial t}$$

The radial profiles developed in the present paper demonstrate specific structural possibilities, but they do not yet constitute such a complete solution.

Similarly, the integrated Maxwell-stress calculation provides a quantitative indicator of radial balance, but a complete dynamical

treatment requires all components of the Maxwell stress tensor together with the time dependence of electromagnetic momentum.

### 9.7. Parameters to Be Determined Experimentally

Several quantities introduced by the model remain undetermined.

They include the characteristic saturated amplitudes,

$$E_0, \qquad B_0$$

the saturated transverse radius,

$$R_0$$

the outer-boundary thickness,

$$\Delta R = R_{\text{out}} - R_0$$

the geometrical energy factor,

$$\text{C}$$

the structural reorganization time,

$$t_{\text{reorg}}$$

and the possible critical convergence angle,

$$\theta_c$$

A reproducible finite transverse scale, a systematic relation between $R_0^2$ and W, or a persistent structural change appearing at a characteristic overlap condition would provide quantitative constraints for further development of the model. [4], [5], [7]

## 10. Conclusions

The present paper extends the conceptual electromagnetic-wave model introduced in Part B1 by examining several mechanisms that may determine the transverse structure, stability, interaction, and measurable dimensions of an electromagnetic wave.

The first result concerns the outer boundary.

The model proposes that a longitudinal displacement current in the inner part of the wave may be accompanied by an oppositely directed displacement-current contribution in an outer annular region. If the integrated displacement current approaches zero at the outer radius,

$$\int_0^{R_{\text{out}}} J_{D,z}(r)\, r\, dr = 0$$

then the corresponding azimuthal magnetic field may also approach zero outside the structure.

This provides a possible electromagnetic mechanism for a strongly limited magnetic field without introducing a material boundary.

The second result concerns radial stability.

The electric and magnetic fields are not assumed to possess identical radial profiles. Near the outer boundary, the magnetic field becomes strongly nonlinear because it must decrease toward zero. The electric field may also become increasingly nonlinear as the local electromagnetic energy density rises.

The competition between these radial field structures can be expressed through the Maxwell stress distribution.

The model proposes that an undersaturated structure is dominated by an inward radial tendency, while an oversaturated structure develops an outward radial tendency.

The saturated condition corresponds to approximate balance.

$$R = R_0$$

At this radius, the characteristic field amplitudes are approximately

$$E = E_0$$

and

$$B = B_0$$

The saturated state is therefore interpreted as a dynamically regulated transverse configuration rather than as an externally imposed boundary.

A third result concerns the interaction between separate electromagnetic-wave structures.

Ordinary overlap produces interference through linear superposition. If the overlap is short, the waves are expected to separate again without permanent structural change.

However, the model proposes that sufficiently long constructive overlap can create a temporarily oversaturated common region.

The suggested sequence is

$$\begin{aligned}\text{overlap} &\rightarrow \text{interference} \rightarrow \text{oversaturation}\\ &\rightarrow \text{radial expansion}\\ &\rightarrow \text{possible merging}\end{aligned}$$

The transition from temporary interference to structural merging is therefore associated with a characteristic overlap time.

$$t_{\text{overlap}} \gtrsim t_{\text{bind}}$$

For nearly parallel waves, the overlap time increases approximately as

$$t_{\text{overlap}} \sim \frac{2R_0}{c\theta}$$

This leads naturally to the concept of a critical convergence angle,

$$\theta_c \sim \frac{2R_0}{ct_{\text{bind}}}$$

below which prolonged coupling may become possible.

If two saturated structures merge while approximately preserving the characteristic saturated amplitudes, their energies add while the transverse radius increases.

For geometrically similar structures at the same wavelength,

$$W = C\lambda\varepsilon_0 E_0^2 R^2$$

and therefore

$$R \propto \sqrt{W}$$

For two equal structures,

$$R_3 = \sqrt{2}R_0$$

while repeated merging of N equal structures gives

$$R_N = \sqrt{N}R_0$$

The model therefore interprets increasing electromagnetic-wave energy primarily as growth of transverse dimension rather than as an unlimited permanent increase of the characteristic saturated field amplitudes.

This interpretation also makes the model experimentally accessible.

A double-slit arrangement may be used to search for a finite transverse scale.

In the simplest symmetric geometry,

$$R_{\text{det}} \approx \frac{d_{max}}{2}$$

where $d_{max}$ presents the largest effective slit separation associated with a measurable common field contribution.

The same geometry can be used to study the convergence angle,

$$\theta = 2\arctan\left(\frac{d}{2L}\right)$$

or, for small angles,

$$\theta \approx \frac{d}{L}$$

Measurements performed at different slit separations and propagation distances may therefore constrain both the transverse radius and the characteristic coupling angle.

The model also provides several more direct experimental predictions.

If saturation exists, increasing electromagnetic-wave energy should produce systematic transverse growth.

$$W \uparrow \Rightarrow R_0$$

For comparable saturated structures,

$$R_0^2 \propto W$$

should approximately hold at fixed wavelength and field geometry.

The outer boundary should also possess a measurable thickness,

$$\Delta R = R_{\text{out}} - R_0$$

which may be constrained through the transition of interference visibility as slit separation is varied.

Several important theoretical problems remain unresolved.

The most important is the construction of a complete three-dimensional source-free Maxwell solution that simultaneously produces finite transverse confinement, a return displacement-current region, a sharply suppressed external magnetic field, longitudinal propagation, energy continuity, and radial stability.

The saturation mechanism also requires a complete treatment of the Maxwell stress tensor and electromagnetic momentum.

These unresolved questions do not prevent the model from producing experimentally testable consequences, but they define the principal mathematical tasks for further development.

The central result of Part B2 is therefore that the proposed transverse electromagnetic structure can be connected to measurable quantities.

The outer boundary, saturated radius, energy-radius relation, overlap time, and critical convergence angle are not only conceptual parameters. They can in principle be constrained by experiment.

Part B1 introduced the electromagnetic wave as a continuous three-dimensional physical structure. Part B2 develops possible mechanisms by which such a structure may acquire a limited outer field, maintain transverse stability, grow through energy accumulation, and interact with neighboring electromagnetic waves.

Together, these results provide a framework for moving from a qualitative structural model toward quantitative experimental verification.

## References


[1] Jackson, J. D. (1998). *Classical Electrodynamics*, 3rd ed. John Wiley & Sons.

[2] Griffiths, D. J. (2023). *Introduction to Electrodynamics*, 5th ed. Cambridge University Press.

[3] Born, M., & Wolf, E. (1999). *Principles of Optics: Electromagnetic Theory of Propagation, Interference and Diffraction of Light*, 7th expanded ed. Cambridge University Press.

[4] Mandel, L., & Wolf, E. (1995). *Optical Coherence and Quantum Optics*. Cambridge University Press.

[5] Goodman, J. W. (2015). *Statistical Optics*, 2nd ed. John Wiley & Sons.

[6] Siegman, A. E. (1986). *Lasers*. University Science Books.

[7] Saleh, B. E. A., & Teich, M. C. (2019). *Fundamentals of Photonics*, 3rd ed. John Wiley & Sons.

[8] Allen, L., Beijersbergen, M. W., Spreeuw, R. J. C., & Woerdman, J. P. (1992). Orbital angular momentum of light and the transformation of Laguerre-Gaussian laser modes. *Physical Review A*, 45(11), 8185–8189. https://doi.org/10.1103/PhysRevA.45.8185